

Formation of an End-On Ferric Peroxo Intermediate upon One-Electron Reduction of a Ferric Superoxo Heme

Jin-Gang Liu, Yuta Shimizu, Takehiro Ohta, and Yoshinori Naruta*

Institute for Materials Chemistry and Engineering, Kyushu University, Higashi-ku, Fukuoka 812-8581, Japan

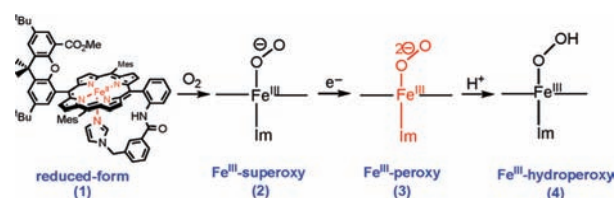
Received January 15, 2010; E-mail: naruta@ms.ifoc.kyushu-u.ac.jp

Activation of molecular oxygen by heme-containing enzymes such as cytochrome P450,^{1a} nitric oxide synthase (NOS),^{1b} and heme oxygenase^{1c} generally involves one-electron reduction of a ferric superoxo adduct to produce a nucleophilic end-on ferric peroxo intermediate. The first of two specific protonations generates the ferric hydroperoxo intermediate (compound 0), while for cytochrome P450 and NOS, the second protonation leads to scission of the O–O bond and formation of a highly reactive oxoferryl species (compound I). In addition to the wide recognition of the oxoferryl species as the active oxidant, there is increasing evidence to suggest that the ferric peroxo species works as an alternative reactive intermediate in the catalytic cycles of NOS and cytochrome P450.^{2,3} Because of its transient character, the isolation and spectroscopic characterization of such ferric peroxo species in heme-containing enzymes have only been achieved using γ -ray or synchrotron X-ray cryoreduction techniques with samples frozen at 77 K, where the first proton delivery is hindered.^{4,5}

Ferric peroxo porphyrin model complexes have been the focus of studies as mimics of the enzymatic ferric peroxo intermediate of biological systems.⁶ However, all of the previously reported ferric peroxo model compounds exhibit the common characteristics of a high-spin state and a side-on binding configuration. These are in sharp contrast to the low-spin end-on counterpart observed during the catalytic cycles of heme enzymes. As part of our continuous efforts to develop models of heme-containing enzymes, we have reported a series of peroxo-bridged heme-(O₂²⁻)-copper peroxides⁷ and recently described the formation of a heme-hydroperoxo compound [(TMPIIm)Fe^{III}-OOH] by proton-coupled electron reduction of the corresponding ferric superoxo precursor.⁸ However, the preparation of the unprotonated low-spin end-on peroxo species from the TMPIIm model using the reduction method has been unsuccessful. In order to further optimize the model compound, we synthesized **1** containing a bulky xanthene substituent that hangs over the porphyrin macrocycle (Scheme 1),⁹ which may provide suitable steric hindrance to protect the “naked” peroxo moiety, thereby stabilizing it in solution. In this report, we describe our success in the preparation of an end-on low-spin ferric peroxo heme intermediate in solution through a one-electron reduction of its ferric superoxo precursor. The obtained ferric peroxo intermediate was further transformed into the corresponding ferric hydroperoxo species upon protonation, as characterized by UV-vis, electron spin resonance (ESR), and resonance Raman (rR) spectroscopies. This ferric peroxo heme intermediate is an “individual” end-on low-spin ferric peroxide that is not coupled to other transition-metal ions and not protonated. This species represents the first example of this type of heme model reported to date.

Introduction of O₂ to a solution of **1** in 20% MeCN/THF at –30 °C readily produced a dioxygen adduct **2** with UV-vis features ($\lambda_{\text{max}} = 428, 550, \text{ and } 592 \text{ nm}$; Figure S1 in the Supporting Information) resembling those of our previously reported ferric superoxo intermediate derived from a cytochrome *c* oxidase model

Scheme 1



($\lambda_{\text{max}} = 425, 550, \text{ and } 590 \text{ nm}$).^{7b} The rR spectra of **2** display an isotope-sensitive band only at 582 (¹⁶O)/556 (¹⁸O) cm⁻¹ in the low-frequency region (Figure S2), which is assignable to the Fe–O₂ stretching vibration of a heme superoxide species. The observed $\nu(\text{Fe}–\text{O}_2)$ frequency is somewhat higher than those of hemoproteins and other heme models ($\nu_{\text{Fe}–\text{O}_2} = 570–576 \text{ cm}^{-1}$)¹⁰ but similar to those of previously reported heme superoxide species generated from twin-coronet porphyrin models.¹¹

After formation of ferric superoxo **2** in solution, excess O₂ was removed, and one-electron reduction was carried out. Addition of 1 equiv of cobaltocene (CoCp₂) to the resultant solution of **2** at –70 °C immediately produced a new species, **3**. The electronic absorption spectra of **3** exhibit absorption maxima at 430, 568, and 610 nm (Figure 1A). These UV-vis features are different from those of side-on peroxo species, whose Soret bands appear at much longer wavelengths,^{6c,8} but similar to those of peroxyoglobin (peroxy-Mb) generated by synchrotron X-ray-irradiated oxy-Mb crystals ($\lambda_{\text{max}} \approx 428 \text{ and } 567 \text{ nm}$).⁵ In addition, the ESR spectra of **3** clearly reveal a low-spin ferric species with small dispersion of *g*-tensor components ($g = [2.27, 2.16, 1.96]$; Figure 1A inset). This result is in good agreement with that of ESR measurements of end-on ferric peroxo heme intermediates generated in enzymes by cryoreduction methods (e.g., for hemoglobin, $g \approx [2.26, 2.14, 1.96]$)^{4b} and sets it apart from ESR data for side-on ferric peroxo compounds, which are characterized by a rhombic high-spin ferric signal at $g \approx 4.2$.^{6,8} The characterization of **3** was further corroborated by rR spectroscopy. The rR spectra of **3** demonstrate two sets of isotope-sensitive bands (Figure 1B). One band appears at 808 cm⁻¹ and shifts to 771 cm⁻¹ upon ¹⁸O substitution. This 808 cm⁻¹ band is assignable to the O–O stretching vibration of a peroxo species. Another band at 585 (¹⁶O)/560 (¹⁸O) cm⁻¹ in the low-frequency region is then assigned to the Fe–O stretching vibration of the corresponding peroxo species. The observed $\nu(\text{O}–\text{O})$ frequency is similar to that of the side-on peroxide species [(TMPIIm)Fe^{III}(O₂²⁻)]⁻ ($\nu_{\text{O}–\text{O}} = 807 \text{ cm}^{-1}$).⁸ The $\nu(\text{Fe}–\text{O})$ frequency, however, is significantly shifted upward from 475 cm⁻¹ for the high-spin species to 585 cm⁻¹ for the low-spin peroxo compound. The observed $\nu(\text{O}–\text{O})$ and $\nu(\text{Fe}–\text{O})$ frequencies of **3** are close to those of our previously reported low-spin peroxo-bridged heme-(O₂²⁻)-copper peroxide complexes ($\nu_{\text{O}–\text{O}} \approx 803 \text{ and } 787 \text{ cm}^{-1}$; $\nu_{\text{Fe}–\text{O}} \approx 611 \text{ cm}^{-1}$).^{7b} On the basis of these experimental results, it can be concluded that one-electron reduction

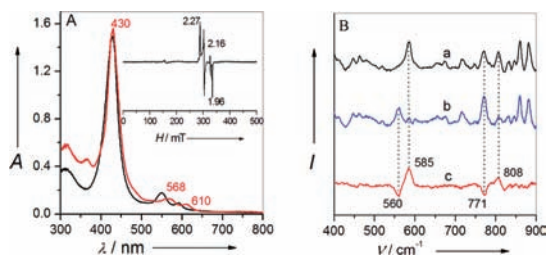


Figure 1. (A) UV-vis spectra of **3** (red line) generated by addition of cobaltocene to the solution of **2** (black line) in 20% MeCN/THF at -70 °C. Inset: ESR spectrum of **3** at 77 K. (B) rR spectra ($\lambda_{\text{ex}} = 413$ nm, 77 K) of **3** containing (a) ^{16}O and (b) ^{18}O and (c) their difference spectrum (a–b).

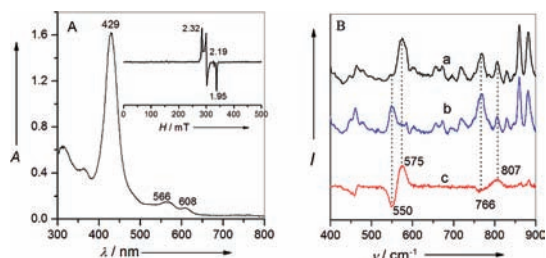


Figure 2. (A) UV-vis spectrum of **4** generated by addition of methanol to the solution of **3** in 20% MeCN/THF at -70 °C. Inset: ESR spectrum of **4** at 77 K. (B) rR spectra ($\lambda_{\text{ex}} = 413$ nm, 77 K) of **4** containing (a) ^{16}O and (b) ^{18}O and (c) their difference spectrum (a–b).

of ferric superoxo **2** in solution readily generates the corresponding end-on low-spin ferric peroxo **3**.

The assignment of **3** as a ferric peroxide was further supported by its tendency to form the corresponding ferric hydroperoxo species upon protonation. Addition of methanol (400 equiv) to a solution of **3** in 20% MeCN/THF at -70 °C affords **4**, which exhibits UV-vis characteristics ($\lambda_{\text{max}} = 429$, 566, and 508 nm; Figure 2A) similar to those of its precursor **3**. The ESR spectrum of **4** (Figure 2A inset) reveals a minor increase in the spread of the g values ($g = [2.32, 2.19, 1.95]$) relative to that of **3**. These results agree well with those of previously reported hydroperoxo heme intermediates from both a model compound⁸ and hemoglobin enzymes ($g \approx [2.32, 2.19, 1.95]$).^{4b} Further characterization of **4** was provided by rR spectroscopy. The rR spectra display isotope shifts of 807 (^{16}O)/766 (^{18}O) cm^{-1} in the region near 800 cm^{-1} and 575 (^{16}O)/550 (^{18}O) cm^{-1} in the low-frequency region (Figure 2B). Deuterium substitution of **4** using MeOD produced a 2 cm^{-1} upshift of the $\nu(\text{O}-\text{O})$ band and a 3 cm^{-1} downshift of the $\nu(\text{Fe}-\text{O})$ band (Figure S3). These H/D substitution shifts are in agreement with previously reported rR data for metallohydroperoxo species and consistent with the existence of hydrogen bonding with the $-\text{OOH}$ moiety.¹² Consequently, the vibrational modes at 807 and 575 cm^{-1} are assigned to the $\nu(\text{O}-\text{O})$ and $\nu(\text{Fe}-\text{O})$ stretching vibrations of the hydroperoxide species, respectively. Protonation of ferric peroxo **3** to yield ferric hydroperoxo **4** causes $\nu(\text{Fe}-\text{O})$ to decrease by 10 cm^{-1} , whereas $\nu(\text{O}-\text{O})$ is not significantly affected. This could be an indication that the added methanol molecules may associate with both the $-\text{OOH}$ and axial imidazole moieties by means of hydrogen bonding. This hydrogen bonding may weaken the electron back-donation from the axial imidazole to the antibonding oxygen π^* orbital of the hydroperoxide in **4**. As a result, the generally expected inverse correlation between an increase in the value of $\nu(\text{Fe}-\text{O})$ and a decrease in the value of $\nu(\text{O}-\text{O})$ upon protonation of a peroxo to yield the corresponding hydroperoxo intermediate becomes less

straightforward with this model system. Nevertheless, the observed $\nu(\text{O}-\text{O})$ and $\nu(\text{Fe}-\text{O})$ values are similar to those of a previously reported $[(\text{TMPIm})\text{Fe}^{\text{III}}-\text{OOH}]$ complex ($\nu_{\text{O}-\text{O}} = 810$ cm^{-1} ; $\nu_{\text{Fe}-\text{O}} = 570$ cm^{-1})⁸ and also comparable to those of the hydroperoxo intermediate isolated from cytochrome P450 by cryoreduction ($\nu_{\text{O}-\text{O}} = 799$ cm^{-1} ; $\nu_{\text{Fe}-\text{O}} = 559$ cm^{-1}).^{12b}

In conclusion, a transient end-on low-spin ferric peroxo heme intermediate derived from a heme model featuring both a group hanging over the porphyrin macrocycle and a covalently appended axial imidazole ligand has been successfully captured in solution for the first time. Steric hindrance provides stabilization of the “naked” peroxy heme in a manner similar to a counteraction or a hydrogen-bonding interaction. This heme model provides a convenient system for sequential preparation of the important and biologically relevant superoxo/peroxo/hydroperoxo heme intermediates through a one-electron reduction/protonation process similar to the mechanisms used by enzyme systems. The results of these proposed investigations will provide a benchmark for characterization and assignment of important peroxo/hydroperoxo heme intermediates.

Acknowledgment. This work was financially supported by Grants-in-Aid for Scientific Research (S) (17105003 to Y.N.) and Young Scientists (B) (27150173 to J.-G.L.) from JSPS and on Priority Areas (19027044 to Y.N.) and Innovative Areas (20200050 to J.-G.L.) from MEXT as well as by the Elemental Science and Technology Project of MEXT.

Supporting Information Available: Experimental details. This material is available free of charge via the Internet at <http://pubs.acs.org>.

References

- (1) (a) Jin, S.; Bryson, T. A.; Dawson, J. H. *J. Biol. Inorg. Chem.* **2004**, *9*, 644. (b) Stuehr, D. J. *Biochim. Biophys. Acta* **1999**, *1411*, 217. (c) Unno, M.; Mastui, T.; Ikeda-Saito, M. *Nat. Prod. Rep.* **2007**, *24*, 553.
- (2) (a) Woodward, J. J.; Chang, M. M.; Martin, N. I.; Marletta, M. A. *J. Am. Chem. Soc.* **2009**, *131*, 297. (b) Gantt, S. L.; Denisov, I. G.; Grinkova, Y. V.; Sligar, S. G. *Biochim. Biophys. Res. Commun.* **2009**, *387*, 169.
- (3) (a) Vaz, A. D. N.; Pernecky, S. J.; Raner, G. M.; Coon, M. J. *Proc. Natl. Acad. Sci. U.S.A.* **1996**, *93*, 4644. (b) Lee-Robichaud, P.; Shyadehi, A. Z.; Wright, J. N.; Akhtar, M. E.; Akhtar, M. *Biochemistry* **1995**, *34*, 14104.
- (4) (a) Davydov, R.; Satterlee, J. D.; Fujii, H.; Sauer-Masarwa, A.; Busch, D. H.; Hoffman, B. M. *J. Am. Chem. Soc.* **2003**, *125*, 16340, and references cited therein. (b) Leibl, W.; Nitschke, W.; Huttermann, J. *Biochim. Biophys. Acta* **1986**, *870*, 20.
- (5) (a) Unno, M.; Chen, H.; Kusama, S.; Shaik, S.; Ikeda-Saito, M. *J. Am. Chem. Soc.* **2007**, *129*, 13394. (b) Hersleth, H. P.; Hsiao, Y. W.; Ryde, U.; Gorbitz, C. H.; Andersson, K. K. *Biochem. J.* **2008**, *412*, 257.
- (6) (a) Wertz, D. L.; Valentine, J. S. *Struct. Bonding (Berlin)* **2000**, *97*, 37, and references cited therein. (b) Durr, K.; Macpherson, B. P.; Warratz, R.; Hampel, F.; Tuczek, F.; Helmreich, M.; Jux, N.; Ivanovic-Burmazovic, I. *J. Am. Chem. Soc.* **2007**, *129*, 4217. (c) Chufan, E. E.; Karlin, K. D. *J. Am. Chem. Soc.* **2003**, *125*, 16160. (d) Goto, Y.; Wada, S.; Morishima, I.; Watanabe, Y. *J. Inorg. Biochem.* **1998**, *69*, 241.
- (7) (a) Liu, J.-G.; Naruta, Y.; Tani, F. *Chem.-Eur. J.* **2007**, *13*, 6365, and references cited therein. (b) Liu, J.-G.; Naruta, Y.; Tani, F. *Angew. Chem., Int. Ed.* **2005**, *44*, 1836.
- (8) Liu, J.-G.; Ohta, T.; Yamaguchi, S.; Ogura, T.; Sakamoto, S.; Maeda, Y.; Naruta, Y. *Angew. Chem., Int. Ed.* **2009**, *48*, 9262.
- (9) Chang, C. J.; Chng, L. L.; Nocera, D. G. *J. Am. Chem. Soc.* **2003**, *125*, 1866. We covalently incorporated an axial imidazole ligand onto the reported “hangman” porphyrin.
- (10) (a) Hirota, S.; Li, T.; Phillips, G. N.; Olson, J. S.; Mukai, M.; Kitagawa, T. *J. Am. Chem. Soc.* **1996**, *118*, 7845. (b) Oertling, W. A.; Kean, R. T.; Wever, R.; Babcock, G. T. *Inorg. Chem.* **1990**, *29*, 2633.
- (11) Tani, F.; Matsu-ura, M.; Ariyama, K.; Setoyama, T.; Shimada, T.; Kobayashi, S.; Hayashi, T.; Matsuo, T.; Hiseada, Y.; Naruta, Y. *Chem.-Eur. J.* **2003**, *9*, 862.
- (12) (a) Kitagawa, T.; Ondrias, M. R.; Rousseau, D. L.; Ikeda-Saito, M.; Yonetani, T. *Nature* **1982**, *298*, 869. (b) Mak, P. J.; Denisov, I. G.; Victoria, D.; Makris, T. M.; Deng, T.; Sligar, S. G.; Kincaid, J. R. *J. Am. Chem. Soc.* **2007**, *129*, 6382. (c) Denisov, I. G.; Mak, P. J.; Makris, T. M.; Sligar, S. G.; Kincaid, J. R. *J. Phys. Chem. A* **2008**, *112*, 13172.

JA1001955